



Theoretical model of absorption coefficient of an inhomogeneous MPP absorber with multi-cavity depths

Ali Ibrahim Mosa^{a,b}, Azma Putra^{c,*}, Roszaidi Ramlan^c, Iwan Prasetyo^d, Al-Ameri Esraa^a

^a *Fakulti Kejuruteraan Mekanikal, Universiti Teknikal Malaysia Melaka, Hang Tuah Jaya, 76100 Durian Tunggal, Melaka, Malaysia*

^b *Mechanical Engineering Department, Collage of Engineering, University of Baghdad, Jadriyah, Baghdad, Iraq*

^c *Centre for Advanced Research on Energy, Universiti Teknikal Malaysia Melaka, Hang Tuah Jaya, 76100 Durian Tunggal, Melaka, Malaysia*

^d *Adhiwijogo Acoustic Laboratory, Department of Engineering Physics, Faculty of Industrial Technology, Institut Teknologi Bandung, Ganesha 10, Bandung 40132, Indonesia*

ARTICLE INFO

Article history:

Received 14 August 2018

Received in revised form 9 October 2018

Accepted 2 November 2018

Keywords:

Micro-perforated panel

Absorption coefficient

Acoustics

Inhomogeneous MPP

ABSTRACT

Micro-perforated panel (MPP) absorber has been known as an alternative absorber to classical porous material given its facile installation, long durability, environmental friendliness and attractive appearance. Extensive studies of MPP absorber proposing the improvement of its absorption frequency bandwidth have been published. This study presents a MPP absorber introduced with inhomogeneous perforations and with multi-cavity depths. The MPP is divided into two sub-area, where each area has different hole diameter, perforation ratio and a separated backed cavity depth. The acoustic impedance is modelled using electrical equivalent circuit and the absorption coefficient is calculated under normal-incidence of sound. It is found that the inhomogeneous MPP can have good bandwidth of absorption by designing the sub-MPP of smaller perforation ratio with large hole diameter and the one having the larger perforation ratio with smaller hole diameter. The absorption bandwidth can be conveniently controlled by adjusting the cavity depth of each sub-MPP. The results from the experimental work show good agreement with the theoretical model.

© 2018 Elsevier Ltd. All rights reserved.

1. Introduction

Studies on micro-perforated panel (MPP) absorber are still progressing. Positioned as the next generation sound absorber, the MPP is often compared with the conventional mineral and synthetic fibrous materials, especially for applications that requires fibre-free materials.

Proposed by Maa in 1975 [1–3], the MPP absorber has been implemented on various acoustics and noise control schemes [4–10]. It differs from the conventional fibrous material, like rockwool and glass-wool, where these materials pose environment and health issues due to the mineral and synthetic substances.

The MPP can be constructed from any kind of thin panels and hence it can offer attractive and aesthetic appearances, including a transparent absorbing panel [11]. The panel must be introduced with sub-millimetric holes backed by an air cavity gap to generate similar Helmholtz resonator mechanism for sound absorption. However, for this original MPP, its absorption frequency bandwidth is naturally narrow, thus limits its potential application, particularly in the broadband sound field naturally present in room

acoustics. Hence, some studies have been proposed to improve its frequency bandwidth by means of structural arrangements or by optimizing its perforation properties.

For the basic structure of MPP, considering a uniform air cavity gap behind the panel, a single Helmholtz resonator mechanism exists which results a single peak covering a narrow frequency range in the absorption coefficient. The absorption amplitude depends on the chosen perforation parameters, ensuring that the acoustic energy undergoes intensification through the sub-millimetric holes [12]. Theoretically, wider absorption bandwidth can be obtained by introducing ultra-micro perforation as suggested by Maa [3] and later proved experimentally by Qian et al. [13]. It should be noted that such MPP specification requires special manufacturing technology and material.

Alternatively, broadband absorption characteristic can be recovered by introducing multiple peaks at different frequencies. This implies a set of different MPPs to be arranged in the MPP absorber system. This kind of system can be realized by arranging the MPPs in series arrangement [14–16], and parallel arrangement [17–19]. The set of overlapped peaks can form a wide absorption bandwidth and the experimental works have been shown to confirm such approaches.

* Corresponding author.

E-mail address: azma.putra@utem.edu.my (A. Putra).

Modifying the backed cavity has also been proposed to enhance the absorption and insulation performances of MPP absorber. This includes by introducing irregular cavity shape [20], by partitioning the cavity [21,22], by introducing parallel-arranged extended tubes [23] and by introducing mechanical impedance plate [24,25].

The works on MPP combined with porous absorptive materials have also been presented, including absorptive materials set in parallel array with a single MPP and with extended tubes having different backed cavity depths [26–31]. Although this structure exhibits improved acoustic performance in the low-to-mid frequency region, however the use of porous material in MPP actually defines a new class of absorber in which absorption mechanism of the system is not solely depending on the resonance of the system. Moreover, such a system is not free from fibrous materials which deviates from the purpose of ‘alternative green absorber’.

From a practical point of view, the series arrangement of MPP is a good choice for the sake of installations on site. However, this approach requires large space because the presence of multiple air cavity that support each MPP layer. Alternatively, a set of different MPPs can be arranged in parallel in which one panel surface consists of several sub-MPPs and where all sub-MPPs share the same cavity depth. Hence, this arrangement does not require additional space for installation. Such an approach has been known as inhomogeneous perforation and the results have been shown to improve the absorption bandwidth of the absorber [32]. However, there exists a limitation to only introducing variation on the perforation parameters (hole size and perforation ratio). In Ref. [32], since the cavity is uniform for all the sub-MPPs, the resonance frequency of each sub-MPP is mainly controlled by adjusting the perforation ratio of each sub-MPP by which the surface impedance is then affected and the absorption amplitude could be lower (as a trade-off to improve the absorption bandwidth).

This research now extends the inhomogeneous perforation approach by introducing a different cavity depth for each set of the sub-MPP as an additional variable parameter to control the absorption bandwidth. This study reports the results of sound absorption coefficient for different combinations of the MPP parameters. The effect of each parameter in this multi-cavity approach on absorption performance is briefly discussed. This study is expected to be part of the design guide when designing the proposed inhomogeneous MPP absorbers with multi-cavity depths.

To realize the concept, mathematical models in Ref. [32] are revised to include the multi-cavity depth and inhomogeneous perforation parameters altogether by using the basic formulation proposed by Maa [3] in which electrical equivalent circuit framework is used to predict the absorption of the system. The model is governed for the case of normal incidence of sound. The performance of the MPP presented in this paper is discussed for the working frequency of 100 Hz up to 1.6 kHz. For other applications, the working frequency can be conveniently adjusted to the lower or higher frequency range by controlling the cavity depth of each sub-MPP.

2. Governing equations

2.1. Acoustic impedance

The acoustic impedances of the micro-perforated panel (MPP) absorber were first proposed by Maa [1], which consist of resistive part and imaginary part. The former corresponds to the resistive force between the fluid and the inner surface of the hole and the latter deals with the inertia force (motion) of the fluid in the hole. The impedances of the MPP are given by:

$$Z_{\text{MPP}} = Z_{\text{resistance}} + Z_{\text{reactance}} = r + j\omega m \quad (1)$$

$$r = \frac{32\eta t}{\rho_0 c_0 d^2 p} \left(\sqrt{1 + \frac{x^2}{32}} + \frac{xd\sqrt{2}}{8t} \right) \quad (2)$$

$$m = \frac{t}{\rho c_0} \left(1 + \left(9 + \frac{x^2}{2} \right)^{-1/2} + \frac{0.85d}{t} \right) \quad (3)$$

$$x = \frac{d}{2} \sqrt{\frac{\omega \rho}{\eta}} \quad (4)$$

where the terms r and m are the normalized specific acoustic resistance and the normalized specific acoustic reactance, respectively, ρ is the density of air, c is the speed of sound wave, ω is the angular frequency, t is the panel thickness, p is the perforation ratio, d is the diameter of the holes and η is the viscosity of air.

The MPP is usually located in front of a rigid surface with an air cavity depth D to maximize the sound absorption mechanism. The impedance of the air cavity is given by Ref. [2]

$$Z_D = -j \cot \left(\frac{\omega D}{c} \right) \quad (5)$$

2.2. Inhomogeneous MPP with multi-cavity depth

Fig. 1(a) shows the schematic diagram of the proposed inhomogeneous MPP absorber model which comprises a finite panel of two areas each with different hole sizes, perforation ratios and backed by two different partitioned air-cavity depths. This area is called ‘sub-MPP’ throughout the rest of this paper. The backed air-cavity depth can be adjusted via altering of the backing rigid wall in the cavity.

The MPP is also assumed to be acoustically rigid to disregard the vibration effect of the panel under acoustic loading. The impinging sound wave on the structure is at normal incident.

The mathematical model based on the electrical equivalent circuit is as depicted in Fig. 1(b). The specific acoustic impedances for each sub-MPP are

$$Z_1 = r_1 + j\omega m_1 + Z_{D1} \quad (6)$$

$$Z_2 = r_2 + j\omega m_2 + Z_{D2} \quad (7)$$

The total acoustic impedance of the inhomogeneous MPP absorber system is expressed as [17]

$$Z_{\text{tot}} = 1 / \left(\frac{a_1}{Z_1} + \frac{a_2}{Z_2} \right) \quad (8)$$

where $a_1 = A_1/A_T$ and $a_2 = A_2/A_T$ are the ratio of the area of the first sub-MPP, A_1 and second sub-MPP, A_2 respectively to the total area of the panel A_T . Note that Eq. (8) does not include the impedance discontinuity between sub-MPPs as discussed in Ref. [33].

The total sound absorption coefficient is given by

$$\alpha = \frac{4\text{Re}\{Z_{\text{tot}}\}}{[1 + \text{Re}\{Z_{\text{tot}}\}]^2 + [\text{Imag}\{Z_{\text{tot}}\}]^2} \quad (9)$$

3. Parametric study

3.1. Effect of inhomogeneous pattern

The introduction of inhomogeneous pattern is to create mixed acoustic impedance on the surface of the MPP system. In this study, the two sets of different impedances are created by an MPP with two parts of area, each part has a different hole diameter, perforation ratio and a backed air cavity. The incoming sound thus perceives the MPP system as having two independent acoustic

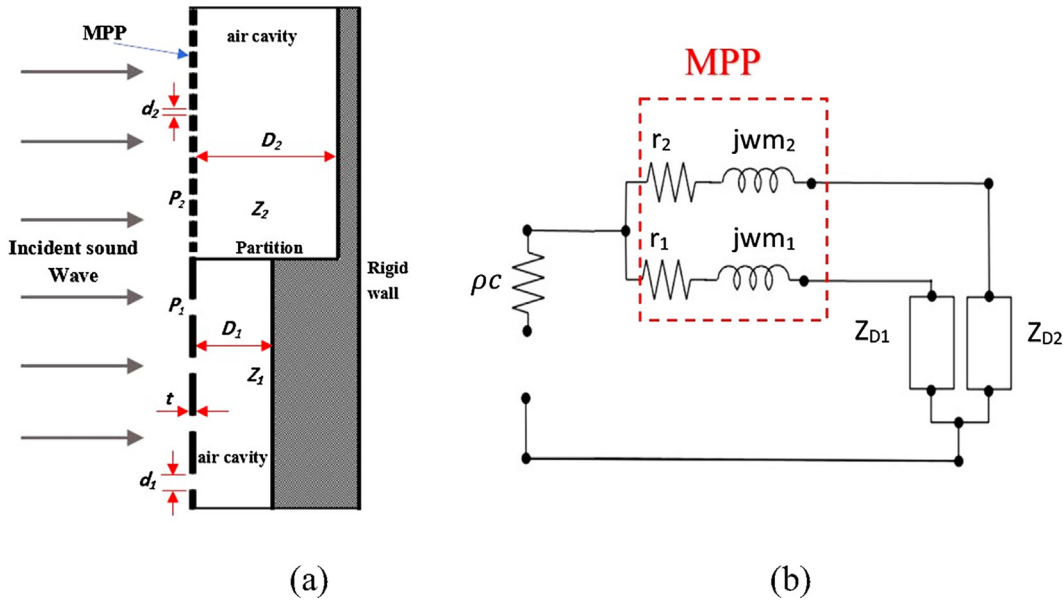


Fig. 1. (a) Schematic diagrams of the inhomogeneous MPP and (b) the electrical equivalent circuit model.

resonators which have a different resonant frequency. The combination of the impedances thus yields a broader frequency bandwidth of absorption. In Ref. [17], it was discussed that there should be the effect of the impedance discontinuity on the MPP surface which affects the absorption coefficient results. However, according to the authors' knowledge, there are still no studies to discuss this in more details, especially those presenting the verification of the hypothesis by experiment. We therefore neglect the effect of the impedance discontinuity in our model. In this section, we present how the inhomogeneous pattern can further improve the bandwidth of the absorption of MPP absorber.

Fig. 2 shows the absorption coefficient of two single MPPs and the inhomogeneous MPP combined from the combination of the two single MPPs. Fig. 2(a) shows the inhomogeneous MPP system, but with a uniform air gap. The improvement of frequency bandwidth as well as the absorption amplitude can be observed clearly. This system has been discussed in detail in Ref. [32], however as shown in Fig. 2(b), the bandwidth towards higher frequency can be improved by introducing a different sub-cavity for each part of the half-area of the inhomogeneous MPP (proposed model in Fig. 1, Eqs. (8) and (9)).

Fig. 2(c) shows the absorption coefficient of the MPP system having a uniform hole size and perforation (homogeneous MPP) with a different sub-cavity (as proposed in Ref. [17]) compared with that of the inhomogeneous MPP with a different sub-cavity (proposed model in Fig. 1). For the latter, the absorption bandwidth can be seen to be significantly wider than the MPP with homogeneous perforation.

The following sections discuss the parametric study of the inhomogeneous MPP and their effects on the sound absorption.

3.2. Effect of perforation ratio

Figs. 3 and 4 presents the absorption performance of inhomogeneous MPP absorbers with different perforation ratios. This is performed for the case where the hole diameter is different for each sub-MPP as demonstrated in Fig. 2(c). The effect of perforation on the sound absorption are simulated by maintaining the perforation ratio of one sub-MPP and by varying the perforation ratio of the other sub-MPP. The general trends can be observed from the results, where wideband frequency can be performed from the variation of perforation ratio difference between the sub-MPP. It

should be noted that the chosen perforation ratio determines the resonance frequency (peak frequency) of the corresponding sub-MPP. The approximate resonance frequency (in kHz) of each sub-MPP can be calculated by Ref. [2]

$$f_0 = \sqrt{\frac{p}{t} \left(\frac{c}{8\pi D} \right)} \quad (10)$$

where p is the perforation ratio specified in % and t and D are the thickness and the cavity depth specified in mm, respectively and $c = 344$ m/s is the speed of sound. Eq. (10) shows that the resonance frequency is proportional to the perforation ratio and in Fig. 3(a)–(c) for examples, it is obvious to observe that the resonance frequency for sub-MPP-1 (p_1 varied) increases as the perforation ratio is increased.

Therefore, for the realization of a wide frequency bandwidth of absorption, the MPP absorber can be designed where the sub-MPPs have separated resonance frequency f_0 and the combination of bandwidth for each sub-MPP forms a wider bandwidth for the inhomogeneous MPP absorber. However, by lowering the value of perforation ratio to shift one resonance frequency to the lower frequency results in lower amplitude of absorption coefficient. Moreover, the dip forming between the two peaks which degrades the amplitude of the absorption must also be compromised.

For example, in Fig. 3(c), large difference of perforation ratio between the sub-MPP ($p_1 = 0.2\%$, $p_2 = 4\%$) demonstrates a distinct peak at the lower frequency (in this case at around 320 Hz, $\alpha = 0.62$) and a high peak at higher frequency (at 1.2 kHz, $\alpha = 0.95$). Between these two resonances, a dip at 550 Hz is formed and the amplitude is low, i.e. $\alpha = 0.2$. As the perforation ratio of the sub-MPP-1 is increased (the difference of the perforation ratio becomes smaller), the amplitude of the lower resonance frequency increases and it shifts to a higher frequency approaching the resonance at 1.2 kHz. By considering the half-absorption bandwidth [2] (i.e. where $\alpha \geq 0.5$), the perforation of $p_1 = 0.6\%$, $p_2 = 4\%$, thus provides the most optimum frequency bandwidth in Fig. 3 (c). As p_1 is increased, the bandwidth becomes narrower, but the overall amplitude of absorption is improved especially as the amplitude of the dip between the two resonances is also increased.

The same phenomenon can also be observed in Fig. 4 for the variation of perforation ratio for sub-MPP-2. The bandwidth can be seen to improve towards higher frequency as the perforation p_2 is increased (for $p_2 > p_1$).

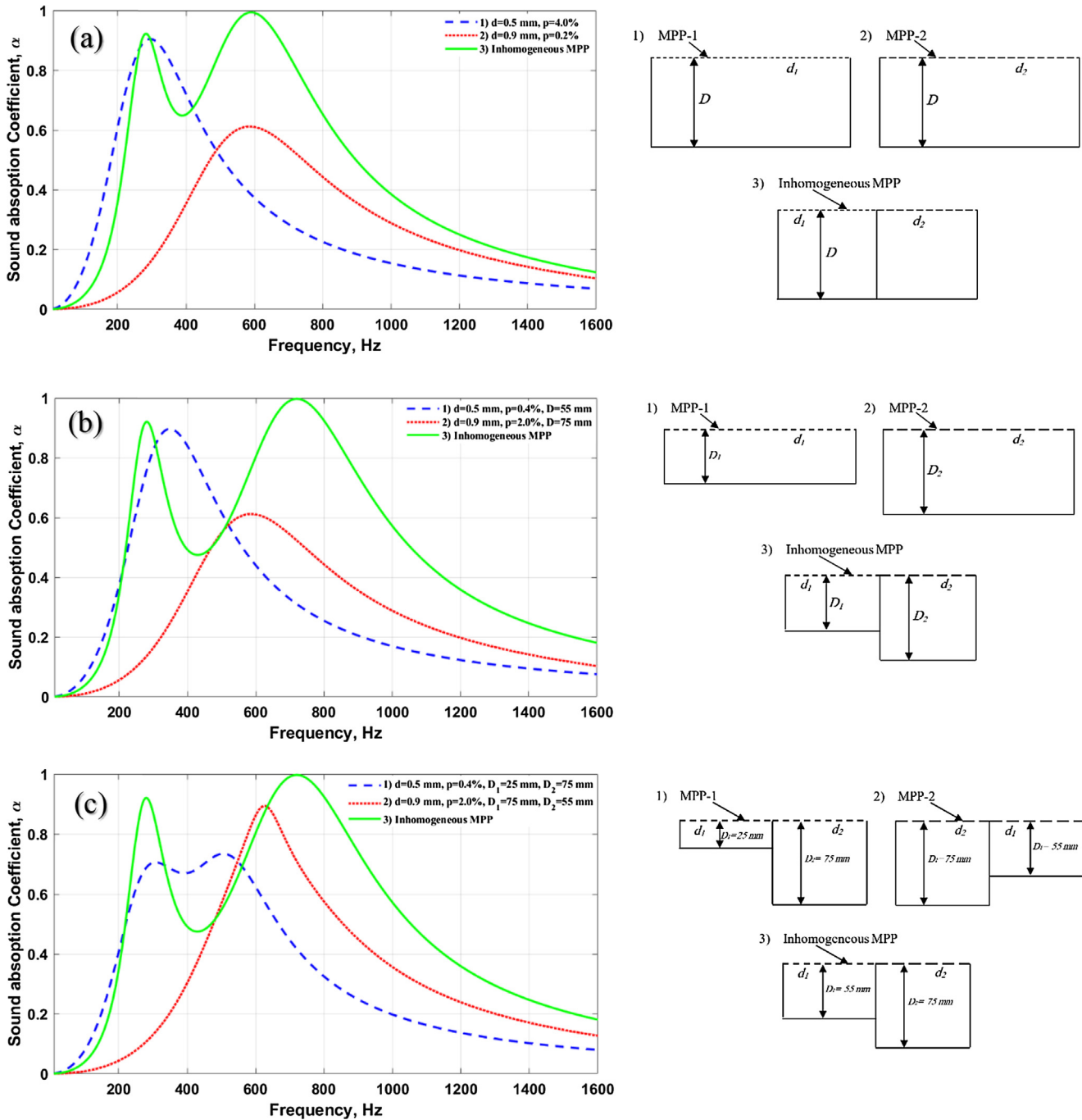


Fig. 2. Comparison of absorption coefficient of: (a) inhomogeneous MPP (uniform cavity, as in Ref. [32]) with homogeneous single MPP, (b) inhomogeneous MPP (multi-cavity) with homogeneous single MPP and (c) inhomogeneous MPP (multi-cavity) with homogeneous MPP (multi-cavity, as in Ref. [17]).

3.3. Effect of hole diameter

In this section, the hole diameter is varied while maintaining the perforation ratio on each sub-MPP. The perforation ratios of $p_1 = 0.6\%$ and $p_2 = 4\%$ are chosen to have the absorption curve with two distinct resonance frequency as in Fig. 3.

Fig. 5 shows the results of the absorption coefficient which was performed by maintaining the diameter of the holes for one sub-MPP, d_2 to be constant (for $p_2 = 4\%$) and the diameter of the other sub-MPP, d_1 is varied (for $p_1 = 0.6\%$). The peak at the lower resonance frequency (in this example is at 550 Hz) increases as the hole diameter d_1 is increased. This creates a better performance of sound absorption. However, the improvement can only be seen

at around the corresponding resonance frequency for a narrow band of frequency.

The amplitude of the corresponding resonance frequency can be calculated from

$$\alpha_{\max} = \frac{4r}{(1+r)^2} \tag{11}$$

where r is the normalized specific acoustic resistance given in Eq. (2).

In Fig. 6, the case was inverted where d_1 is constant (for $p_1 = 0.6\%$) and d_2 is varied (for $p_2 = 4\%$). Contrary to the results shown in Fig. 5, here the absorption coefficient and the frequency bandwidth increases as the diameter d_2 is reduced. The effect on

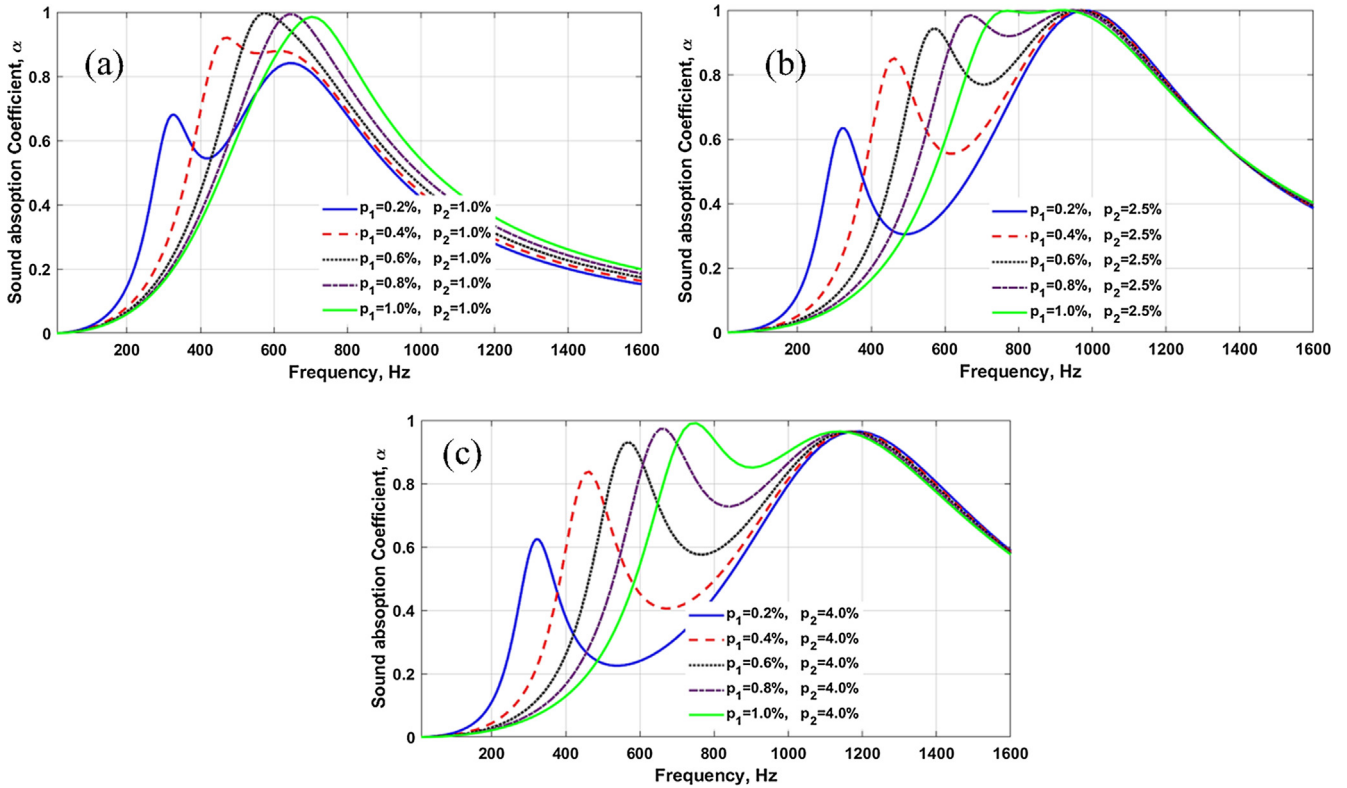


Fig. 3. Effect of perforation ratio on absorption coefficient of the inhomogeneous MPP: $d_1 = 0.8$ mm, $d_2 = 0.4$ mm, and $D_1 = 30$ mm, $D_2 = 40$ mm, $t = 1$ mm (p_1 varied, p_2 fixed).

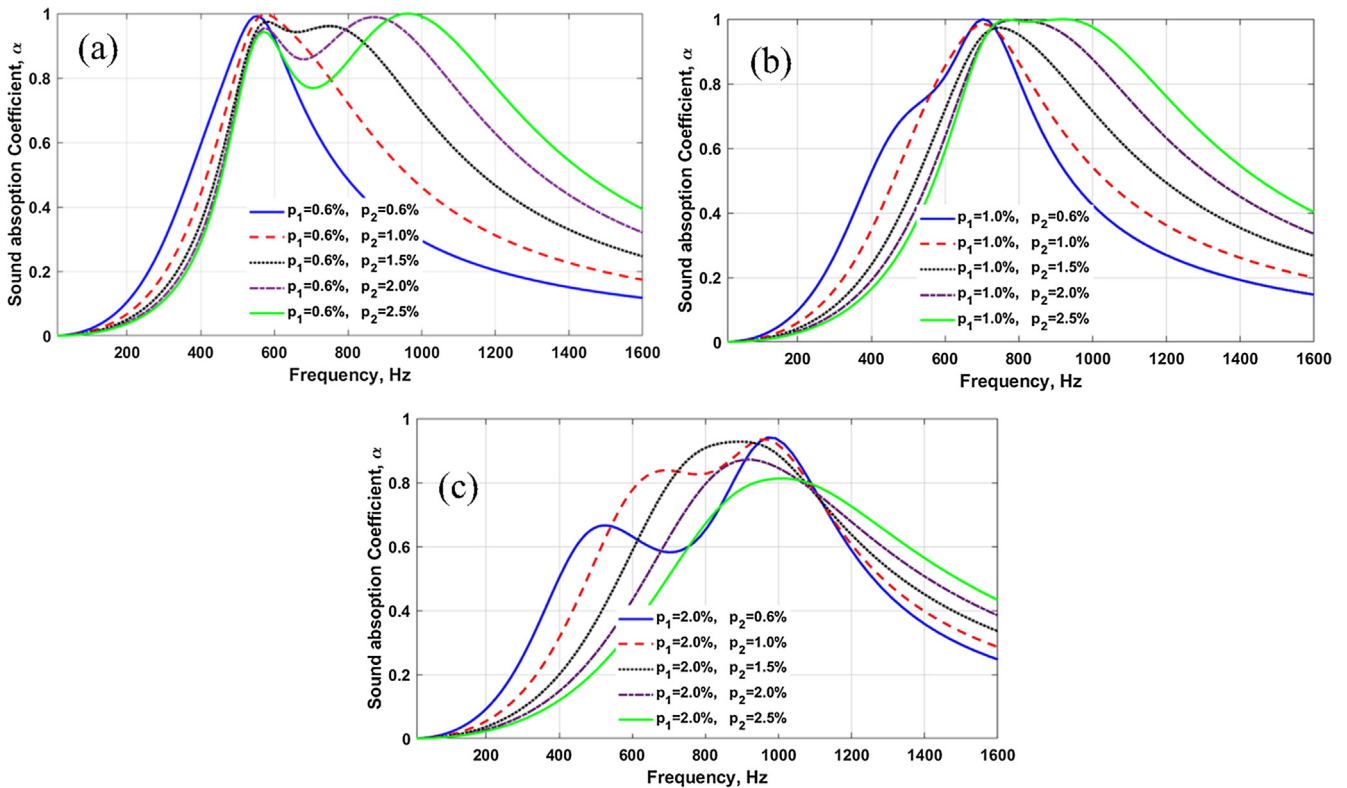


Fig. 4. Effect of perforation ratio on absorption coefficient of the inhomogeneous MPP: $d_1 = 0.8$ mm, $d_2 = 0.4$ mm, and $D_1 = 30$ mm, $D_2 = 40$ mm, $t = 1$ mm (p_1 fixed, p_2 varied).

the bandwidth can be seen to be greater compared to the case in Fig. 5, where here the amplitude at the second resonance (at 1.1 kHz) including the dip (at 750–800 Hz) are improved. This finding suggests that reducing the hole size diameter for the sub-MPP

with the greater perforation ratio provides more significant improvement in terms of the amplitude of absorption coefficient and the frequency bandwidth compared to increasing the hole diameter for the sub-MPP with the smaller perforation ratio.

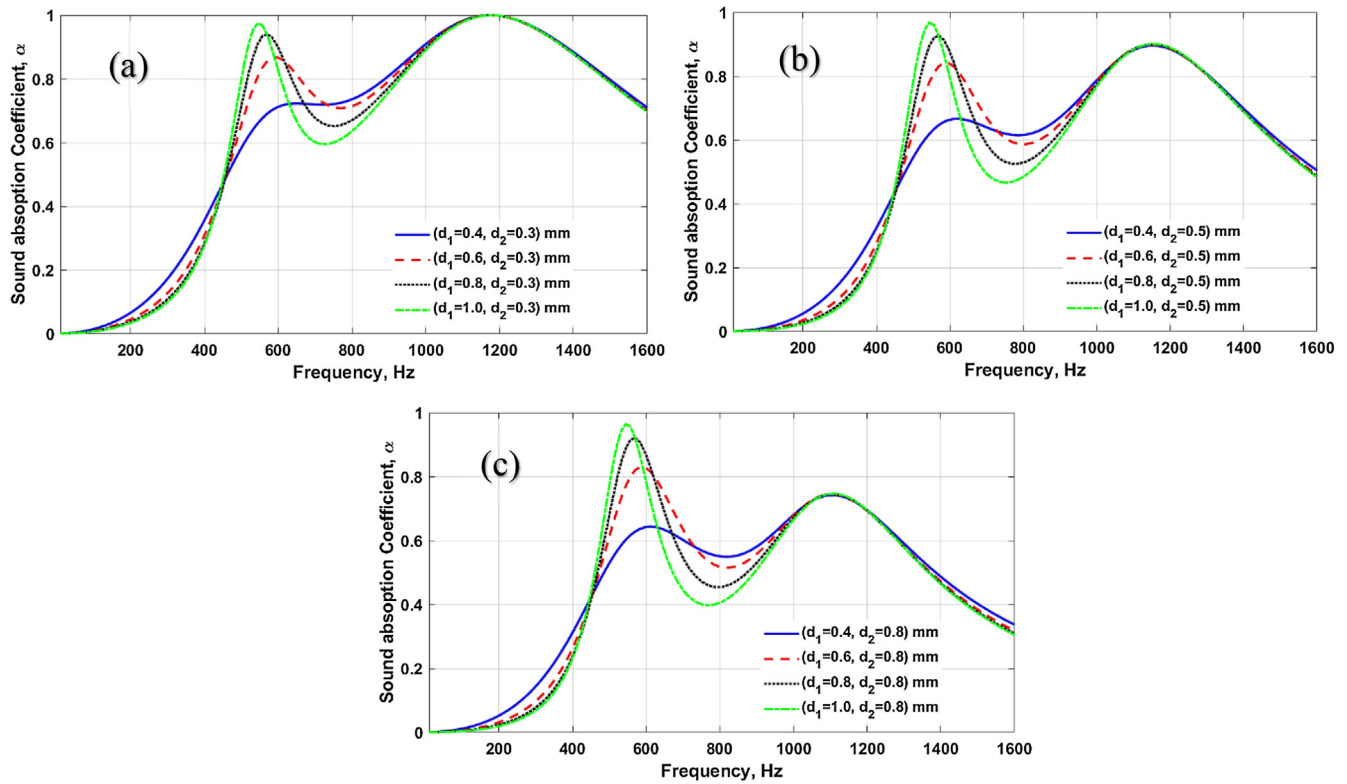


Fig. 5. Effect of hole diameter on absorption coefficient of the inhomogeneous MPP: $D_1 = 30$ mm, $D_2 = 40$ mm, $p_1 = 0.6\%$, $p_2 = 4\%$, $t = 1$ mm (d_1 varied, d_2 fixed).

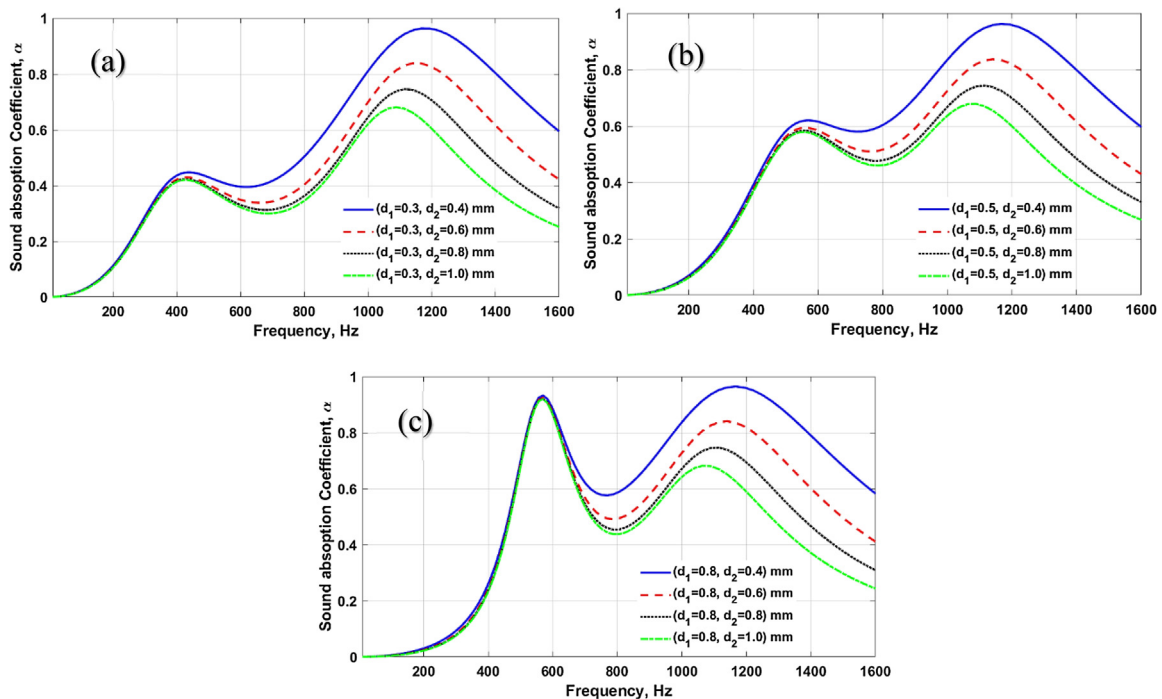


Fig. 6. Effect of hole diameter on absorption coefficient of the inhomogeneous MPP: $D_1 = 30$ mm, $D_2 = 40$ mm, $p_1 = 0.6\%$, $p_2 = 4\%$, $t = 1$ mm (d_1 fixed, d_2 varied).

The results demonstrate that the inhomogeneous MPP must preferably have a feature where the sub-MPP with the smaller perforation ratio to have a few holes with a moderately large diameter and one with the greater perforation ratio to have many holes with moderate small diameter as illustrated in Fig. 7.

3.4. Effect of backed cavity depth

In this study, the inhomogeneous MPP is proposed with the backed air cavity partitioned into two sub-cavities of different depths. Fig. 8 shows the effect of combination of the backed cavity

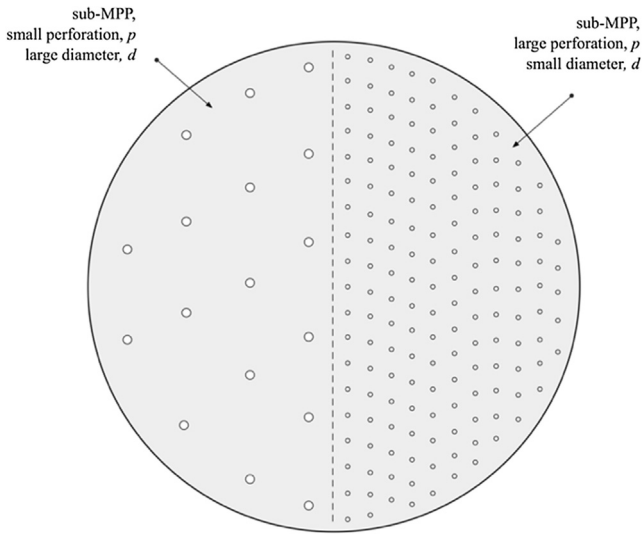


Fig. 7. Illustration of the general features of the inhomogeneous MPP to have an optimum sound absorption performance.

depths for the inhomogeneous MPP. The cavity depth D_1 of sub-MPP-1 is maintained constant and that of the sub-MPP-2, D_2 is varied. The first resonance frequency corresponds to D_1 (also subjected to the perforation ratio of the sub-MPP) and the second resonance frequency at higher frequency corresponds to the variation of D_2 .

It can be observed how the bandwidth of absorption is formed as D_2 is increased where this shifts the second peak to approach the peak of D_1 towards lower frequency (see again Eq. (10)). The desired absorption bandwidth can thus be designed by controlling the difference of the cavity depth between the two sub-MPPs. For example in Fig. 8(a), the MPP with $D_1 = 30$ mm, $D_2 = 40$ mm can

be seen to have a wide half-absorption bandwidth ($\alpha \geq 0.5$) from around 500 Hz–1.6 kHz, compared with that having greater cavity depth of $D_1 = 30$ mm, $D_2 = 70$ mm (thus consumes more space) which provides bandwidth at 500 Hz–1.1 kHz (the latter only performs better to the former at 600–900 Hz).

Fig. 9 shows the results for variation of the cavity depth D_1 while D_2 is kept constant. The first peak can now be observed to shift to the lower frequency as D_1 is increased which improves the absorption bandwidth at lower frequencies. However, as discussed in Section 3.2, the forming of the dip between the two resonance frequencies must be taken care of.

It can also be observed that adjusting the cavity depth to improve the absorption bandwidth only shifts the peak frequency without any reduction on the peak amplitude as what is found by adjusting the perforation ration discussed in Section 3.2. By adjusting the perforation ratio of each sub-MPP, the surface impedance is affected and the absorption coefficient could result in a lower amplitude (as a trade-off to improve the absorption bandwidth). See again Figs. 3 and 4.

4. Experiment

4.1. Materials

The material used to fabricate the MPP samples is the Polyvinyl Chloride normal grade named PVC-U. The material has good mechanical strength, good machining ability, good chemical resistance, very low water absorption (<0.007% per 24 h), easy to varnish and low cost. It has density of 1.42 g/cm³. The PVC can also come with various colors which can make the MPP more attractive.

4.2. Sample fabrication

The MPP samples have diameter of 33 mm to fit the diameter of the impedance tube in the experiment. The cavity case was

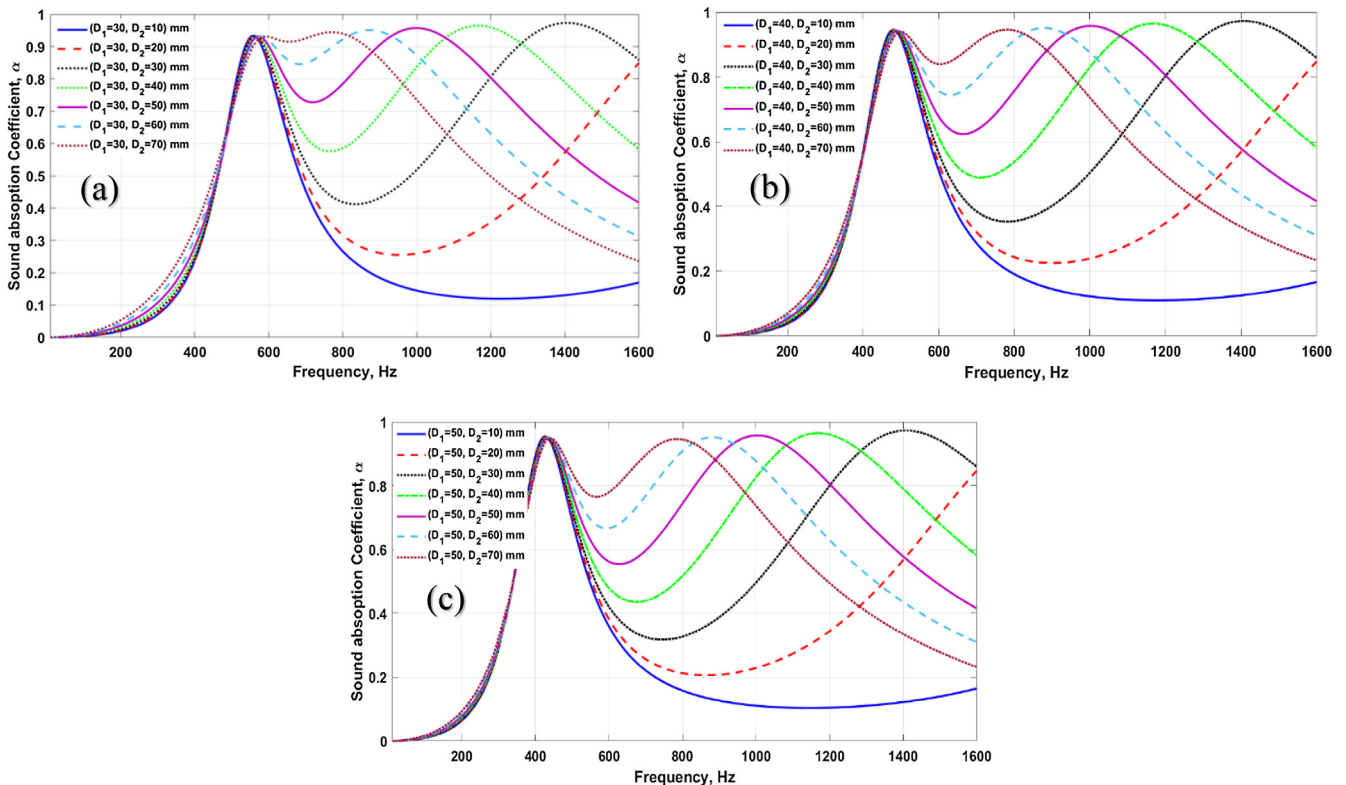


Fig. 8. Effect of cavity depth on absorption coefficient of the inhomogeneous MPP: $d_1 = 0.8$ mm, $d_2 = 0.4$ mm, $p_1 = 0.6\%$, $p_2 = 4\%$, $t = 1$ mm (D_1 fixed, D_2 varied).

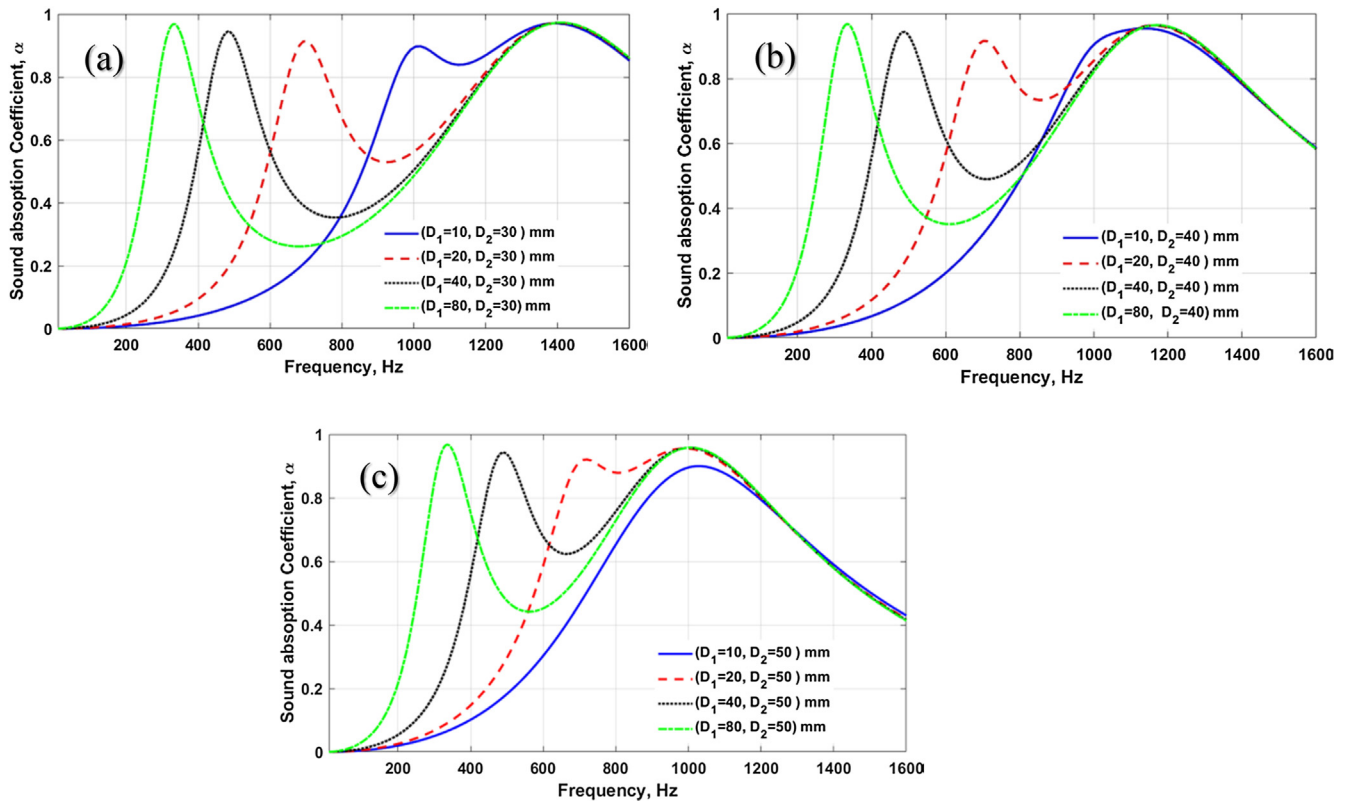


Fig. 9. Effect of cavity depth on absorption coefficient of the inhomogeneous MPP: $d_1 = 0.8$ mm, $d_2 = 0.4$ mm, $p_1 = 0.6\%$, $p_2 = 4\%$, $t = 1$ mm (D_1 varied, D_2 fixed).

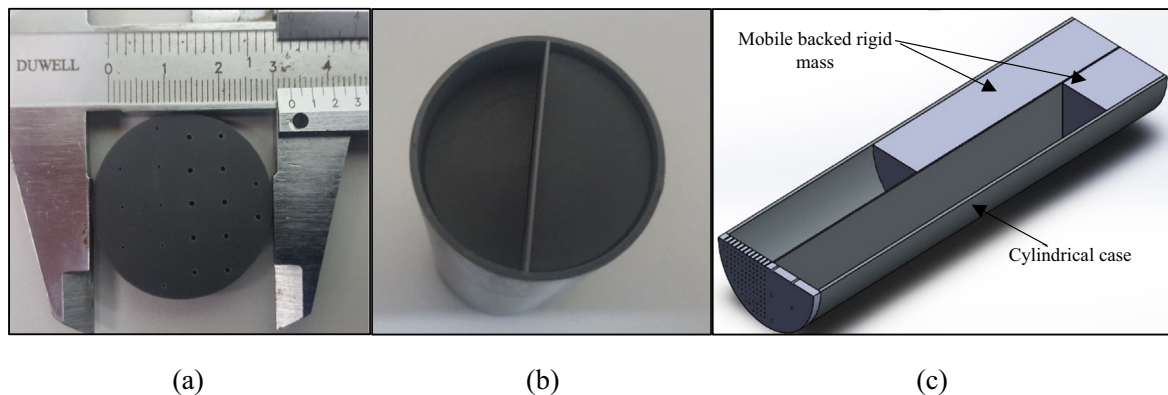


Fig. 10. (a) Inhomogeneous MPP samples size; (b) cylindrical-shaped case with a partition separating the two-cavity (top view) and (c) a two-mobile backed rigid mass (cross section view).

designed as a cylindrical shape with a partition separating the two-cavity and a two-mobile backed rigid mass to control the depth of each cavity. The partition is to ensure the cavity has separate, independent acoustic impedance. See Fig. 10.

The samples of the MPP were designed with two different hole diameters and two different perforation ratios in same panel. The examples are shown in Fig. 11. The structural parameters of these inhomogeneous MPP absorbers (I-MPP) samples used in the experiment are listed in the Table 1.

4.3. Experimental setup and absorption coefficient measurement

The measurement of absorption coefficient was performed by using the impedance tube method having two microphones based

on the transfer function method according to the ISO 10534-2 [34]. The impedance tube has an inner diameter of 33 mm. The sample was set at one end of the impedance tube and it was ensured that the cavity casing was fitted tightly inside the tube leaving almost no gap between the inner surface of the tube and the outer surface of the casing also the sample was in zero level with the vertical axis of the testing impedance tube.

A stationary white noise was generated in the impedance tube through a loudspeaker located at the other end of the tube. Two $\frac{1}{2}$ -in pre-polarised free-field acoustic microphones (GRAS 40AE) with $\frac{1}{2}$ -in CCP pre-amplifier (GRAS 26CA) were used to measure the built-in sound pressure inside the tube. Prior the measurement, the sensitivity of the microphones was calibrated by using Brüel & Kjær sound calibrator type 4231 at 114 dB level and 1 kHz. Data

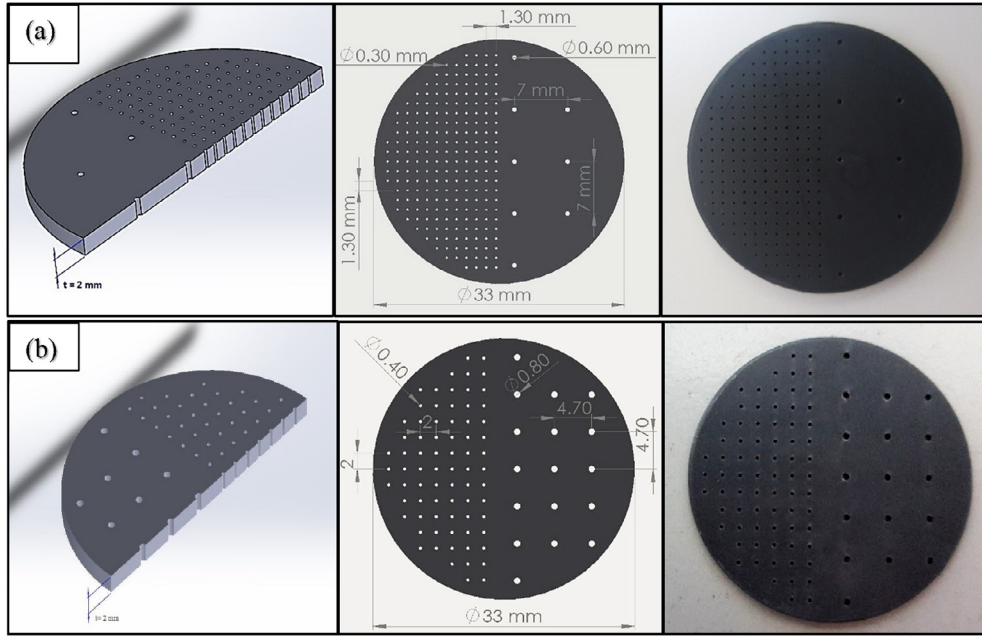


Fig. 11. Schematic diagrams and photos of PVC inhomogeneous MPP absorber: (a) I-MPP-1; (b) I-MPP-2.

Table 1
PVC inhomogeneous MPPs absorbers samples structural parameters.

Sample No.	Sample diameter, (mm)	Panel thickness, t (mm)	Hole diameter 1, d_1 (mm)	Hole diameter 2, d_2 (mm)	Perforation ratio 1, p_1 %	Perforation ratio 2, p_2 %	Hole spacing 1, b_1 (mm)	Hole spacing 2, b_2 (mm)
I-MPP-1	33	2	0.6	0.3	0.6	4.0	7	1.3
I-MPP-2	33	2	0.8	0.4	2.3	2.5	4.7	2

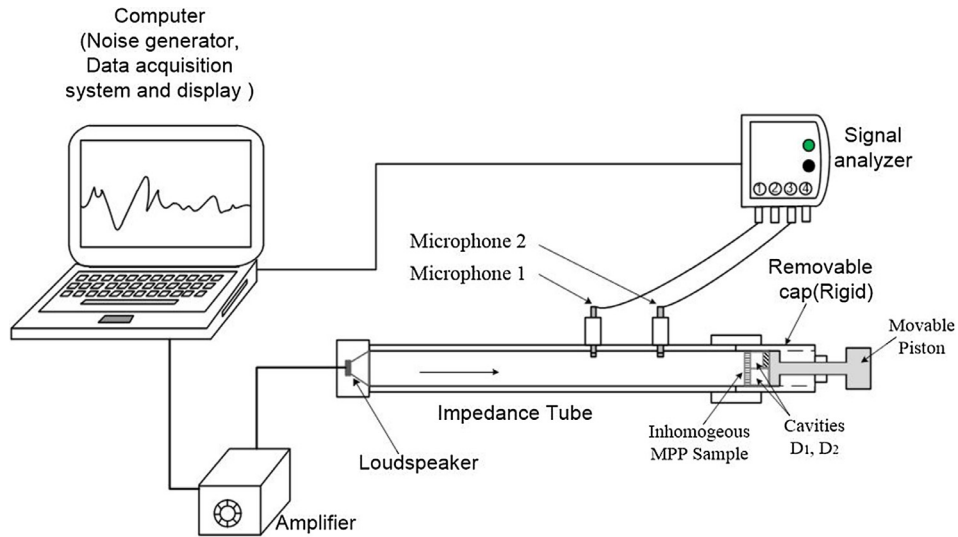


Fig. 12. Diagram of the experimental setup for the normal-incidence absorption coefficient measurement using the impedance tube method.

Physics analyzer was used as the data acquisition system to process the recorded pressure signals. Calculation of the absorption coefficient was performed using MATLAB. Fig. 12 shows the diagram of the experimental setup.

Measurement was conducted for two samples of MPP listed in Table 1 with some variations of cavity depths. For each sample, the test was repeated three times to ensure small variabilities in

the measured results and to obtain the average result of the measured absorption coefficient.

4.4. Measured absorption coefficient

Fig. 13 shows the comparison of the measured absorption coefficient with those from the proposed mathematical model. In gen-

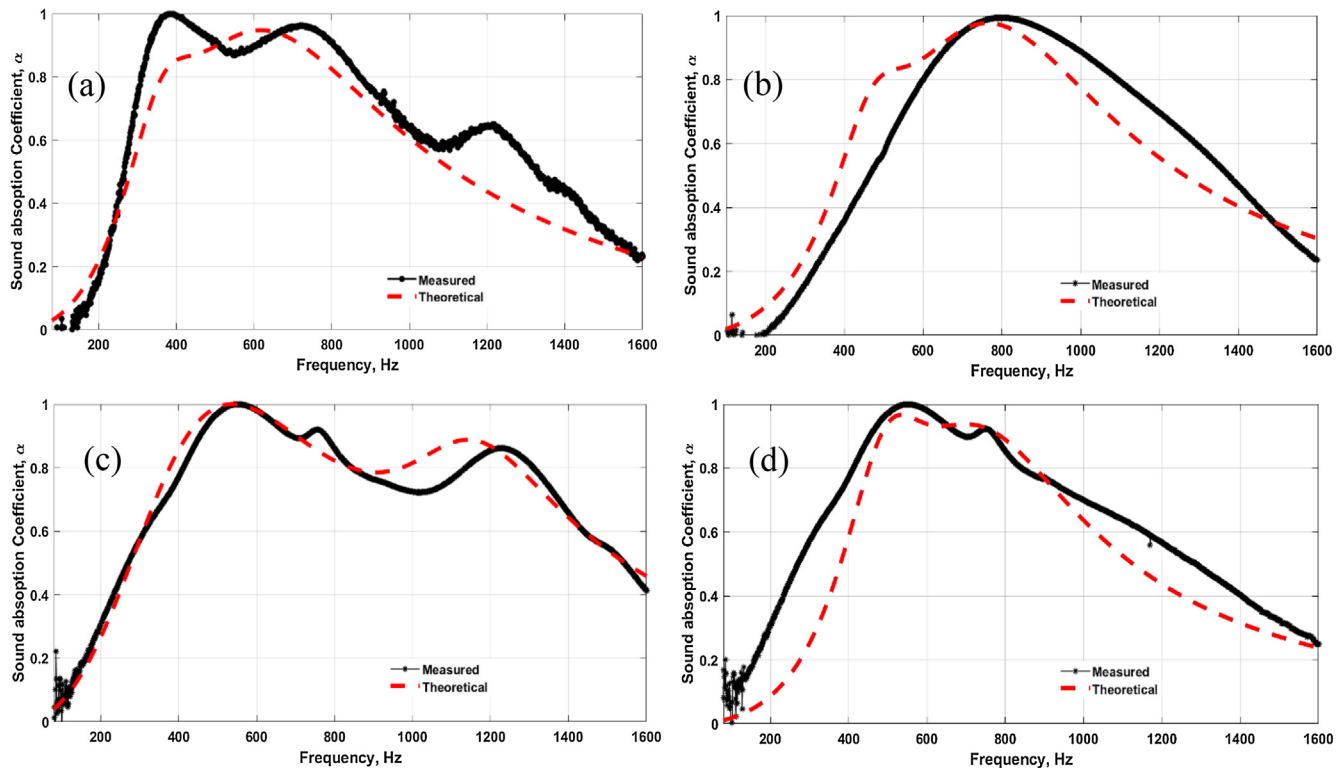


Fig. 13. Comparison of measured absorption coefficient with the theoretical model (Fig. 1, Eqs. (8) and (9)) for: (a) I-MPP-1: $D_1 = 40$ mm, $D_2 = 75$ mm; (b) I-MPP 1: $D_1 = 25$ mm, $D_2 = 55$ mm; (c) I-MPP-2: $D_1 = 75$ mm, $D_2 = 15$ mm and (d) I-MPP 2: $D_1 = 45$ mm, $D_2 = 75$ mm.

eral, a reasonably good agreement can be observed between the theory and the measured results. In Fig. 13(a), the measured data presents peaks at 400 Hz, 700 Hz and 1.2 kHz. Noise can be observed in the measured curve which may be the cause of the inaccuracy. However, the general trend and the frequency bandwidth agree fairly with the model.

Fig. 13(b) also shows good agreement of the measured result with the theory although the former shifts slightly to higher frequency. In Fig. 13(c), the second peak frequency of the measured data is slightly higher than the theoretical. In Fig. 13(d) a good agreement of the measured result with the theory can be observed, although the former shows a slightly wider absorption bandwidth. The effect of surface impedance discontinuity may cause these differences which is neglected in the model, where the inter-play effects between two sub-MPP exist. Other than that, the trend of the measured result agrees well with that of the theoretical model.

5. Conclusion

The absorption coefficient of the inhomogeneous MPP with multi-cavity depths has been discussed. It is shown that introduction of inhomogeneous perforation improves the absorption performance of a MPP absorber compared to the homogenous one, especially with multi-cavity depths. Parametric study by varying the perforation ratio, the hole diameter and the cavity depth has been presented to discuss the phenomena obtained from each parameter changes in improving the absorption coefficient of the inhomogeneous MPP absorber.

The absorption bandwidth can be improved by controlling the perforation ratio difference between the sub-MPPs. The desired bandwidth of absorption with lower and upper resonance frequency, f_0 can be designed using Eq. (10) and with the chosen thickness of MPP, the perforation ratio, p and the cavity depth, D can be obtained. However, reduction of absorption amplitude as

the consequence of changing the surface impedance effect to achieve a wider absorption bandwidth must be taken care of. For this reason, controlling the cavity depth has been shown to be a better option to widen the bandwidth while maintaining the absorption amplitude.

The parametric study also reveals that the optimum absorption performance can be obtained by having one of the sub-MPP with the smaller perforation ratio to have larger diameter of holes (still sub-millimetric size) and the other sub-MPP with the greater perforation ratio to have smaller diameter of holes.

Experimental results from the impedance tube test have been presented where the data have good agreement with the theory.

This report limits the analysis for the inhomogeneous MPP divided into two sub-parts of MPP area. The study can be further extended for more multiple sub-MPPs. It is also of interest to study the performance of MPP system with an additional inhomogeneous MPP layer and a cavity gap creating a double-MPP system to produce wider absorption bandwidth.

Acknowledgements

Part of this project is supported by the Fundamental Research Grant Scheme from Ministry of Higher Education Malaysia No. FRGS/1/2016/TK03/FTK-CARE/F00323.

References

- [1] D., You Maa. Theory and design of microperforated panel sound-absorbing constructions. *Sci Sinica* 1975;18(1):55–71.
- [2] Maa D. Microperforated-panel wideband absorbers. *Noise Control Eng J* 1985, 1987.;29(June):77–84.
- [3] Maa D. Potential of microperforated panel absorber. *J Acoust Soc Am* 1997, 1998.;104(November):2861–6.
- [4] Zha X, Fuchs HV, Drotleff H. Improving the acoustic working conditions for musicians in small spaces. *Appl Acoust* 2002;63(2):203–21.

- [5] Kang J, Brocklesby MW. Feasibility of applying micro-perforated absorbers in acoustic window systems. *Appl Acoust* 2005;66(6):669–89.
- [6] Yu X, Cheng L, You X. Hybrid silencers with micro-perforated panels and internal partitions. *J Acoust Soc Am* 2015;137(February):951–62.
- [7] Yu X, Lau SK, Cheng L, Cui F. A numerical investigation on the sound insulation of ventilation windows. *Appl Acoust* 2017;117:113–21.
- [8] Okuzono T, Sakagami K. Room acoustics simulation with single-leaf microperforated panel absorber using two-dimensional finite-element method. *Acoust Sci Technol* 2015;36(4):358–61.
- [9] Allam S. Optimal design of compact multi-partition MPP silencers for I.C. engines noise control. *Noise Control Eng J* 2016;64(5):615–26.
- [10] Liu D, Du B, Yan M, Wang S. Suppressing noise for an HTS amorphous metal core transformer by using microperforated panel absorber. *IEEE Trans Appl Supercond* 2016;26(7).
- [11] Asdrubali F, Pispola G. Properties of transparent sound-absorbing panels for use in noise barriers. *J Acoust Soc Am* 2007;121(1):214–21.
- [12] Ingard KU. Notes on sound absorption technology. Poughkeepsie, NY: Noise Control Foundation; 1994.
- [13] Qian YJ, Kong DY, Liu SM, Sun SM, Zhao Z. Investigation on micro-perforated panel absorber with ultra-micro perforations. *Appl Acoust* 2013;74(7):931–5.
- [14] Kang J, Fuchs HV. Predicting the absorption of open weave textiles and micro-perforated membranes backed by an air space. *J Sound Vib* 1999;220(5):905–20.
- [15] Sakagami K, Morimoto M, Koike W. A numerical study of double-leaf microperforated panel absorbers. *Appl Acoust* 2006;67(7):609–19.
- [16] Sakagami K, Matsutani K, Morimoto M. Sound absorption of a double-leaf micro-perforated panel with an air-back cavity and a rigid-back wall: detailed analysis with a Helmholtz-Kirchhoff integral formulation. *Appl Acoust* 2010;71(5):411–7.
- [17] Sakagami K, Nagayama Y, Morimoto M, Yairi M. Pilot study on wideband sound absorber obtained by combination of two different microperforated panel (MPP) absorbers. *Acoust Sci Technol* 2009;30(2):154–6.
- [18] Wang C, Huang L, Zhang Y. Oblique incidence sound absorption of parallel arrangement of multiple micro-perforated panel absorbers in a periodic pattern. *J Sound Vib* 2014;333(25):6828–42.
- [19] Wang C, Huang L. On the acoustic properties of parallel arrangement of multiple micro-perforated panel absorbers with different cavity depths. *J Acoust Soc Am* 2011;130(1):208–18.
- [20] Wang C, Cheng L, Pan J, Yu G. Sound absorption of a micro-perforated panel backed by an irregular-shaped cavity. *J Acoust Soc Am* 2010;127(1):238–46.
- [21] Toyoda M, Takahashi D. Sound transmission through a microperforated-panel structure with subdivided air cavities. *J Acoust Soc Am* 2008;124(6):3594–603.
- [22] Liu J, Herrin DW. Enhancing micro-perforated panel attenuation by partitioning the adjoining cavity. *Appl Acoust* 2010;71(2):120–7.
- [23] Li D, Chang D, Liu B. Enhancing the low frequency sound absorption of a perforated panel by parallel-arranged extended tubes. *Appl Acoust* 2016;102:126–32.
- [24] Zhao X, Fan X. Enhancing low frequency sound absorption of micro-perforated panel absorbers by using mechanical impedance plates. *Appl Acoust* 2015;88(October 2017):123–8.
- [25] Zhao XD, Yu YJ, Wu YJ. Improving low-frequency sound absorption of micro-perforated panel absorbers by using mechanical impedance plate combined with Helmholtz resonators. *Appl Acoust* 2016;114:92–8.
- [26] Sakagami K, Kobatake S, Kano K, Morimoto M, Yairi M. Sound absorption characteristics of a single microperforated panel absorber backed by a porous absorbent layer. *Acoust Aust* 2011;39(3):95–100.
- [27] Liu Z, Zhan J, Fard M, Davy JL. Acoustic measurement of a 3D printed micro-perforated panel combined with a porous material. *Meas J Int Meas Conf* 2017;104:233–6.
- [28] Liu Z, Zhan J, Fard M, Davy JL. Acoustic properties of multilayer sound absorbers with a 3D printed micro-perforated panel. *Appl Acoust* 2017;121:25–32.
- [29] Atalla N, Sgard F. Modeling of perforated plates and screens using rigid frame porous models. *J Sound Vib* 2007;303(1–2):195–208.
- [30] Li D, Chang D, Liu B, Tian J. Improving sound absorption bandwidth of micro-perforated panel by adding porous materials. *Inter-noise* 2014;1:1–6.
- [31] Li D, Chang D, Liu B. Enhanced low- to mid-frequency sound absorption using parallel-arranged perforated plates with extended tubes and porous material. *Appl Acoust* 2017;127:316–23.
- [32] Prasetyo I, Sarwono J, Sihar I. Study on inhomogeneous perforation thick micro-perforated panel sound absorbers absorbers. *J Mech Eng Sci* 2016;10(3):2350–62.
- [33] Yairi M, Sakagami K, Takebayashi K, Morimoto M. Excess sound absorption at normal incidence by two microperforated panel absorbers with different impedance. *Acoust Sci Technol* 2011;32(5):194–200.
- [34] International Organization for Standardization. ISO 10534-2, acoustics – determination of sound absorption coefficient and impedance in impedance tubes. *Int. Stand.*; 2001.